LUNAR SURFACE THORIUM ANOMALIES: EVIDENCE FOR CRUSTAL STRATIGRAPHY AND STRUCTURE IN PROCELLARUM KREEP TERRANE (PKT) AND SOUTH POLE-AITKEN TERRANE (SPAT). Jingyi Zhang[1,2], James W. Head[2], Jianzhong Liu[1], Ross W. K. Potter[2,3]. [1]Center for Lunar and Planetary Science, Institute of Geochemistry, Chinese Academy of Sciences, Guiyang 550081, China, email: zhangjiangyi@mail.gyig.ac.cn, [2]Department of Earth, Environmental and Planetary Sciences, Brown University, Providence, RI 02912 USA, [3]Clarivate, 160 Blackfriars Road, London SE1 8EZ UK.

Introduction: Most lunar evolution models predict that fractional crystallization of lunar magma ocean will produce a layer of melt enriched in incompatible elements such as K, REE, and P (i.e., KREEP) [1]. Some workers [2] have proposed that the surficial distribution of Th, which has been measured on a global-scale [3,4,5] can be used as a proxy for determining the global distribution of KREEP. The Th and FeO distribution are also used to divide the lunar surface into three main Terranes: Procellarum KREEP (PKT), Feldspathic Highland (FHT) and South Pole-Aitken (SPAT) [2]. Here we use the boundary of PKT in [6]. There are obvious high-Th abundance locations in the PKT, only medium in parts of SPAT, but almost none in FHT (Fig. 1). The lateral extent and distribution of the "KREEP" layer is currently a matter of debate. Based on the global asymmetry of the Th distribution, some workers suggested that the Procellarum region is the oldest lunar impact basin [7,8], the formation of which may have caused the accumulation of KREEP-rich material on the nearside; in contrast, the farside generally lacks the same high abundances of Th and other KREEPy elements [9,10]. Other mechanisms have been proposed to explain the Th anomalies, including inhomogeneous differentiation of the magma ocean [11], and farside impact basin effects [12].

In this analysis, we use the relations between transient cavity depth or diameter [13] and crater excavation depth given by Potter and Melsoh [14,15] to obtain sampling depth data. We then assess the three-dimensional geometry of Th concentrations in the PKT and compare the relations between PKT and SPA as a basis for an hypothesis to explain Th distribution and characteristics.

Nature of Thorium anomalies in the PKT and SPAT: The Th abundance map (Fig. 1) shows that the high-Th areas in the PKT are 1) mainly related to Imbrium ejecta (Fra Mauro Formation-FMF) and/or post-Imbrium KREEP volcanism in the PKT, and 2) concentrated at the location of young impact craters in mare and highlands regions [16]. We studied several such craters located on highlands and mare regions (Table 1), including Mairan, Kepler, Aristarchus, Aristillus, Copernicus and Plato. In particular, the high-Th concentration regions are near Mairan, Kepler, Aristarchus, and Aristillus. However, Copernicus and Plato, which are located on the FMF and the Imbrium rim respectively, show relatively low Th values. Small craters within Imbrium generally show lower Th abundance than those on the highlands, (suggesting that they are excavating maria, not Th-rich FMF or crust). There are two craters (Atistillus and Timochairs) that show high Th abundances, and appear to excavate through Th-poor maria and into Th-rich Imbrium basin deposits (FMF, etc.) (Fig. 1; Table 1). A second concentration of Th is within Mare Ingenii area in SPA (Fig. 1). This concentration shows peaks at two impact craters, Birkeland (81.4 km diameter) and Oresme V (56.1 km diameter) (Fig. 1, Table 1).

Crustal stratigraphy implied by Th anomalies in PKT and SPAT: There exists a higher Th abundance in PKT than its surrounding areas, which has been interpreted as KREEP materials being mainly concentrated in the subsurface of the PKT [2,6,16,17], perhaps throughout the crust. In the PKT, combining these high-Th craters and their excavation depths (Table 1), we found that craters on the highlands (mostly FMF) show the highest Th abundances, except Copernicus and Plato, the excavation depths of which are deeper than other high-Th locations. We thus interpret the Th concentration to have been excavated by the Imbrium impact and distributed only onto the very shallow surface of the highlands (the FMF), and thus much less abundant at greater depth. There are two craters (Aristillus and Timocharis) that show relatively high Th abundance in Imbrium (Fig. 1), even though the mare is many hundreds of meters thick. We interpret this to mean that they both penetrated through the mare basalts filling the Imbrium basin and excavated underlying Th-rich material of the Imbrium basin floor. Based on these Th anomalies, we have constructed a cross-sectional stratigraphic interpretation of PKT (Fig. 2a). This lends support to the model of the Th rich material being concentrated primarily in Imbrium basin ejecta deposits and related impact melt and KREEP volcanism, independent of the lunar mare fill.

In SPA, observed Th anomalies occur on the central, more mafic floor of the basin and are related to two craters (Fig. 1) suggesting that the origin of the Th is related to excavation and, therefore, likely indigenous [18-19]. We then interpret the stratigraphy of these occurrences (Fig. 2b) to indicate the presence of a lowermost subcrustal KREEP layer in the farside SPAT region, that was brought to the near-surface by removal of much of the overlying crust by the oblique SPA basin event, and then excavated and exposed at the surface by the Birkeland and Oresme impact events that penetrated through the SPA basin interior deposits.

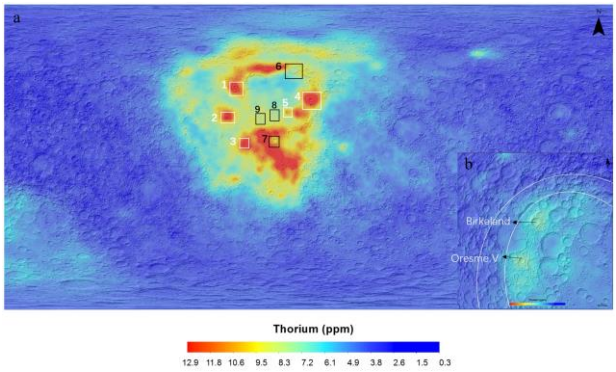

Figure 1 Global thorium abundance from LP gamma-ray spectrometer overlain on LOLA hillshade map. **a)** White and black square boxes show high-Th and low-Th concentrations, respectively. 1-Mairan, 2-Aristarchus, 3- Kepler, 4-Aristillus, 5- Timocharis, 6- Plato, 7-Copernicus, 8-Euler, 9-Lambert. **b)** on the lower right corner: White dashed oval represents SPA area. Birkeland and Oresme V craters in SPA with peak Th abundances.

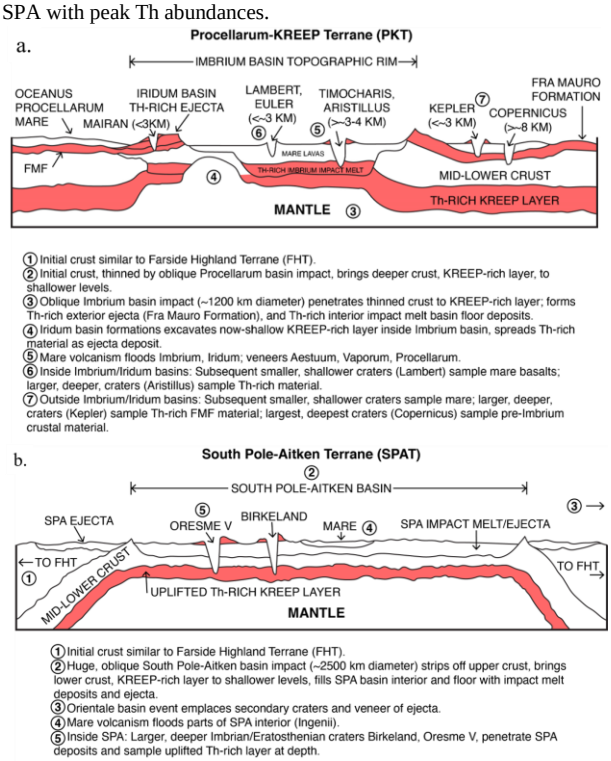

① Initial crust similar to Farside Highland Terrane (FHT).
② Initial crust, thinned by oblique Procellarum basin impact, brings deeper crust, KREEP-rich layer, to shallower levels.
③ Oblique Imbrium basin impact (~1200 km diameter) penetrates thinned crust to KREEP-rich layer; forms Th-rich exterior ejecta (Fra Mauro Formation), and Th-rich interior impact melt basin floor deposits.
④ Iridum basin formations excavates now-shallow KREEP-rich layer inside Imbrium basin, spreads Th-rich material as ejecta deposit.
⑤ Mare volcanism floods Imbrium, Iridum; veneers Aestuum, Vaporum, Procellarum.
⑥ Inside Imbrium/Iridum basins: Subsequent smaller, shallower craters (Lambert) sample mare basalts; larger, deeper, craters (Aristillus) sample Th-rich material.
⑦ Outside Imbrium/Iridum basins: Subsequent smaller, shallower craters sample mare; larger, deeper, craters (Kepler) sample Th-rich FMF material; largest, deepest craters (Copernicus) sample pre-Imbrium crustal material.

① Initial crust similar to Farside Highland Terrane (FHT).
② Huge, oblique South Pole-Aitken basin impact (~2500 km diameter) strips off upper crust, brings lower crust, KREEP-rich layer to shallower levels, fills SPA basin interior and floor with impact melt deposits and ejecta.
③ Orientale basin event emplaces secondary craters and veneer of ejecta.
④ Mare volcanism floods parts of SPA interior (Ingenii).
⑤ Inside SPA: Larger, deeper Imbrian/Eratosthenian craters Birkeland, Oresme V, penetrate SPA deposits and sample uplifted Th-rich layer at depth.

Figure 2. Reconstructed crustal cross-sections in a) PKT and b) SPAT.

Origin of PKT and SPAT Th anomalies: Based on these cross-sectional stratigraphic and geometric relationships (Fig. 2a, b), we interpret the high Th distribution in PKT and SPA to be related to sequential oblique and near-vertical impacts. First, an oblique impact formed a Procellarum basin, removing much of the upper and middle crust in the area and bringing the residual KREEP-rich layer close to the surface. This was followed by formation of the SPA basin by oblique impact [12], similarly removing much of the upper and middle crust and exposing the KREEP-rich lower crust covered by SPA impact melt. Subsequently, the more-vertical Imbrium basin impact penetrated the shallow KREEP layer, ejecting it to form the FMF and related Th-rich ejecta and impact melt deposits. Later mare volcanism buried the KREEP-rich deposits under hundreds of m to km of lava. In the SPA basin, similar vertical impacts Birkeland and Oresme V excavated Th-rich material from below the melt sheet to create the locally high Th anomalies.

In summary, this interpretive scenario 1) attributes the origin of the PKT and SPA Th anomalies to sequential impact processes, requiring no additional mechanisms to concentrate KREEP in the SPA or PKT terrain at depth, in agreement with [20], and 2) suggests the presence of a pre-Imbrium PKT target stratigraphy similar to the current SPAT (compare Figures 2a-b): an upper SPAT like ferroan anorthosite layer overlying a lower KREEP-rich layer. The high-Th materials were thus concentrated primarily in basin ejecta deposits and related impact melt and KREEP volcanism, independent of the later lunar mare fill.

Table 1.

Name	Diameter (km)	Transient cavity diameter [c] (km)	Transient cavity depth [c] (km)	Excavation depth [a](km)	Excavation depth [b] (km)
Euler	26.03	23.96	7.99	2.88	2.66
Kepler	31	26.65	8.88	3.19	2.96
Lambert	30.12	27.13	9.04	3.26	3.01
Timocharis	34.14	30.18	10.06	3.62	3.53
Aristarchus	42	34.52	11.51	4.14	3.84
Marian	34.49	34.15	11.83	4.09	3.94
Aristillus	54.37	44.82	14.94	5.38	4.98
Copernicus	96	72.71	24.24	8.73	8.08
Plato	100.68	75.67	25.22	9.08	8.41
Birkeland	81.64	63.32	21.11	7.59	7.04
Oresme V	56.1	46.03	15.34	5.52	5.11

a, Potter et al. (2015);
b, Melosh (1989);
c, 2015 LPI Impact Crater Database (Croft 1985; Stöffler et al. (2006).
Red craters in Table 1 represent those craters with relatively high Th content in PKT.

References: [1] Warren & Wasson (1979) RGSP 17, 73. [2] Jolliff et al. (2000) JGR 105, 4197. [3] Lawrence et al. (1998) Science 281, 1484. [4] Lawrence et al. (2003) JGR 108, 5102. [5] Lawrence et al. (2007) GRL L03201. [6] Haskin et al. (2000) JGR 205. [7] P. H. Cadogan, 1974, SCIENCE 250 315.[8] Nakamura et al., 2012, NATURE 5, 775.[9] Warren & Kallemeyn (1998) LPI 6408. [10] Zhu et al. (2019) JGR 124, 2117.[11] Loper et al., (2002) JGR,107, 5046.[12] Schultz et al., (2011) GSA SP 477. [13] (http://www.lpi.usra.edu/lunar/surface/). [14] Potter et al. (2015) GSA SP 518, 99. [15] Melosh (1989) 74. [15] Binder (1998) Science 281. 5382. [16] Wieczorek et al. (2000), JGR 105, 20417. [17] Haskin (1998) JGR 103, 1679. [18] Garrick-Bethell et al. (2005), GRL 32, L13203. [19] Moriarty et al. (2021), JGR 121, e2020JE006589. [20] Evans (2019) LPSC 50 #2733.